Decision support for emergency road traffic management in post-earthquake conditions

Pierre Gehl, Samuel Auclair, Rosemary Fayjaloun, Philippe Méresse

International Journal of Disaster Risk Reduction 77 (2022) 103098

Contents lists available at ScienceDirect

International Journal of Disaster Risk Reduction

journal homepage: www.elsevier.com/locate/ijdrr

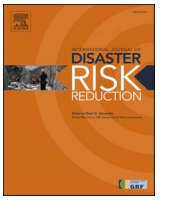

Decision support for emergency road traffic management in post-earthquake conditions

Pierre Gehl [a,*], Samuel Auclair [a], Rosemary Fayjaloun [a], Philippe Meresse [b]

[a] Risks and Prevention Division, BRGM, Orléans, France
[b] Valabre, Gardanne, France

ARTICLE INFO

Keywords:
Earthquake
First response
Road network
Decision support
Uncertainty

ABSTRACT

Road network systems play a critical role in the emergency phase following an earthquake, since they constitute the main vector of transportation of rescue teams, first-aid responders or victims in need of evacuation. While several studies have focused on how to organize multi-agent travels via a traffic plan, the present work focuses on how to immediately help first-aid responders, at a moment when the actual damage state of the road network is still mostly unknown. Therefore, in such an uncertain context, a probabilistic framework is used in order to evaluate the failure probability of exposed road components and the accessibility probability between two locations of the network, via a decomposition into minimum link sets. Such data is then used to extract relevant indicators for each potential travel itinerary, such as the expected travel time (accounting for potential disruptions along the route and the need to use a back-up itinerary) or the reliability of the itinerary and its back-ups. Given predefined road user profiles, with different weightings of indicator preferences, the various travel options may be evaluated in a decision matrix in order to assist the choice of the most adequate itinerary. Finally, such as decision support system is demonstrated on a road network in the Pyrenees mountain range (France), where several travel options (i.e., fastest or safest routes from the damaged area to nearby hospitals, or from rescue centres to the damage area) are evaluated for a few earthquake scenarios and characteristic user profiles.

1. Introduction

The main duties of search and rescue (SAR) teams are to locate, extract and provide initial medical care for victims trapped in rubble after disaster events such as earthquakes. To access the impacted areas, these teams must deal with particularly significant "barrier effects" that can delay their intervention activities, such as the blocking of streets with rubble or crowds of people [1]. Once the rescuers arrive on site, the work of reconnaissance of damaged buildings, the task assignment of the rescue services, and the subsequent identification and extraction of victims under rubble are particularly time-consuming and technically demanding. In addition to the SAR teams, many other first responders must converge towards the impacted area to deploy advanced medical posts (AMPs) that provide on-site initial care, to evacuate casualties requiring urgent care to hospitals as quickly as possible, to ensure security in the affected area, etc. This gradual increase in emergency capacity requires the rapid delivery of new resources to the field, in a context where road networks are often saturated and may be damaged.

Earthquake-induced material damage (physical losses) to infrastructure can have repercussions on the entire transport system, by

* Corresponding author.
E-mail address: p.gehl@brgm.fr (P. Gehl).

https://doi.org/10.1016/j.ijdrr.2022.103098
Received 24 February 2022; Received in revised form 11 May 2022; Accepted 31 May 2022
Available online 3 June 2022

disrupting the connectivity of routes (functional losses), as demonstrated by recent examples. The 2016 Kaikoura (New Zealand) earthquake (M_w 7.8) triggered widespread landslides and ground failures, which led to the destruction of roads and the isolation of many rural settlements. Also in 2016, the Central Italy earthquake sequence (M_w 6.1 and M_w 6.5 events) damaged several road bridges, which required the construction of temporary structures for emergency response and recovery [2]. A road network consists of various assets interacting with the surrounding environment. Efforts to inventory and characterise these assets have been carried out recently [3,4], in parallel to studies focusing on the physical vulnerability of specific road network components [5], such as bridges [6], tunnels [7], road embankments [8] or retaining walls [9]. While roads and tunnels remain relatively unaffected by earthquakes except in the case of permanent ground movements (surface fault rupture, landslides, liquefaction, etc.), bridges are the components that generally suffer the most damage from wave propagation effects [10]. Since the function of these structures is to cross obstacles (rivers, valleys, other roads, etc.) and thus to significantly reduce the travel time, their failure is particularly critical in terms of impact on the performance of the entire infrastructure network.

Based on a literature review of road network vulnerability, El-Maissi et al. [11] have split assessment methods into two categories: the first one encompasses physics-based methods that use fragility functions associated with vulnerability indices, the second one covers traffic-based methods that qualify the accessibility of routes via link importance indices. The study by El-Maissi et al. [11] indicates that a robust evaluation of the effects of earthquakes on road networks requires a coupling of both approaches, so that the functional losses associated with assessed damages account for the physical vulnerability of components. To measure the post-earthquake performance of transportation systems, researchers typically use engineering-based metrics, some of which are summarized in Table 1.

However, in the case of transporting operational resources to the earthquake-impacted area and evacuating victims, these metrics are not sufficient for prioritizing routes according to their ability to satisfy user requirements expressed in terms of minimizing cost functions (in terms of travel time, risk of blockage, etc.). Comprehensive literature reviews in this field can be found in Ref. [19–21]. As a result, this issue is usually addressed using resource allocation optimization techniques in the context of a multi-agent response with a high level of supervision, where a service in charge of coordinating the operational response prioritizes the following items in real-time: “what to send”, “where”, and “by which route”. This could include optimizing the deployment of SAR teams based on a rapid assessment of human casualties [22], the transfer of patients between hospitals based on the effects of the earthquake on the healthcare system [23], or the distribution of humanitarian resources [24]. However, this approach of supervised design of relief logistics networks only becomes feasible once situational awareness increases to the point that authorities can manage to organize a coherent response (which can take several hours up to several days depending on the size of the earthquake and the level of preparedness of the authorities); it is incompatible with the initial post-earthquake phase characterized by a general state of confusion, particularly related to the status of roadways [25]. Thus, contrary to these studies that focus on how to regulate and organize traffic, the present work focuses on how to help first-aid responders, who have to intervene immediately before a traffic plan defining safe routes reserved for emergency services is implemented.

The main issue that is investigated here pertains to the identification of adequate travel solutions in a degraded environment, where only an incomplete view of the actual situation is available. To this end, it is proposed to develop a decision support system (DSS) at the level of a road network, where potential actions (i.e., representing choices of travel routes) are evaluated under uncertain conditions. A similar DSS, applied to a seaport system, has been developed by Cremen et al. [26] in the context of earthquake early warning, where the range of possible actions boils down to “alert” or “no alert”. In the present study, the DSS is used in a rapid response context, which implies a wider perimeter of potential actions. First, the challenges facing various types of users, depending on their respective objectives, are detailed in Section 2, with the objective of identifying a set of road network user profiles. Then, in Section 3, a probabilistic framework for the evaluation of road network damage and accessible travel routes is introduced: from this starting point, it is shown how various indicators may be extracted in order to compare the routes in a decision matrix, which constitutes the basis for the proposed DSS. Finally, the whole approach is demonstrated on a road network in the Pyrenees mountain range (France), where several travel options (i.e., fastest or safest routes from the damaged area to nearby hospitals, or from rescue centres to the damaged area) are evaluated for a few earthquake scenarios and user profiles (Section 4).

2. Operational pitfalls and needs during the initial response phase

From a crisis logistics point of view, the most critical phase after the occurrence of an earthquake is undoubtedly the initial response, which is mainly dominated by the rescue of people and characterized by a state of confusion in relation to traffic flow [27]. The problem can be considered at two different scales:

Table 1
Summary of the most common measures of the post-earthquake performance of road networks.

Performance measure	Reference
Loss of connectivity, quantifies the decrease in the number of origins connected to a destination node	[12]
Additional post-earthquake distance travelled between two locations of interest	[13]
“Travel time delay”, i.e. the cumulative additional time needed to travel due to damage ()	[14,15]
“Disruption index” based on qualitative criteria	[16]
Functional percentage of a road network, considered as a measure of system resilience	[17]
Accessibility, measures the ease with which people can reach given destinations	[18]

1. At the individual level of the agents (rescue workers, police forces, citizens, etc.). The challenge is to choose a route that maximizes their chances of accessing or exiting the impacted area where damage is the most significant, with prioritization criteria specific to each agent (speed of the itinerary, safety, reliability, etc.);
2. At the collective level of the authorities in charge of crisis management. The challenge is to regulate traffic by defining a traffic plan that allows each agent to carry out their mission on adapted routes.

In both cases, it is proposed to build a context-based prioritization of itineraries that accounts for the potential effects of the earthquake in terms of damage as estimated by situational awareness tools. To do so, it is first necessary to consider the overall schematic vision of the main incoming and outgoing flows to/from the impacted area, as represented in Fig. 1:

- Routing of SAR teams within the impacted area:
  - o Urban search and rescue (USAR) teams and their equipment are transported by road to search and extract victims trapped under the rubble;
  - o The relevant emergency team is transported by road to set up AMPs that provide a first level of care;
  - o The relevant emergency team is transported by road to establish emergency accommodation centres that accommodate unharmed but homeless disaster victims.
- Setting up of rotations for the evacuation of seriously injured people requiring urgent hospitalization:
  - o The most critical cases ("absolute emergencies") are evacuated by helicopter, and are thus removed from the system discussed in the following;
  - o Serious cases (and sometimes some of the "absolute emergencies") are evacuated by road using medical ambulances, if their health condition allows it.
- Access of engineering evaluation teams to the most critical structures that affect the usability of the main road route, with the aim of making an initial diagnosis of the measures necessary for reopening.
- Spontaneous movements from the general population, to evacuate the affected area or to provide assistance.

Each of the agents considered in this situation can be described in terms of their own objectives, which are reflected in particular by the timeframe of the transport action, by the direction in relation to the impacted area (in/out) (Table 2), and by the specific criteria for prioritizing itineraries.

3. Situational awareness and initial response phase

In the following sub-sections, a probabilistic tool for the updating of system losses [28] is briefly summarized. Then, the procedure to extract potential choices of itineraries and to organize them in a consequence matrix is detailed with the objective of improved decision making.

3.1. Description of the loss updating procedure for a road network system

Relying on previous developments regarding the post-earthquake loss assessment of infrastructure systems [29–32], a tool using Bayesian updating has been developed by Gehl et al. [28] for rapidly estimating losses to built areas and road networks. A Bayesian Network (BN) is designed with the OpenBUGS tool [33], which enables the modelling of continuous and discrete variables in the same BN. The OpenBUGS library is freely available, integrated in the R (www.r-project.org) environment, and it uses approximate inference via Monte-Carlo Markov-Chain (MCMC) sampling. The developed BN relies on three main types of variables:

- Spatially distributed intensity measure (IM) at the locations of infrastructure components (e.g., road bridges), which represent the distribution of the logarithm of the ground-motion parameter of interest (e.g., peak ground acceleration, PGA). A spatial correlation

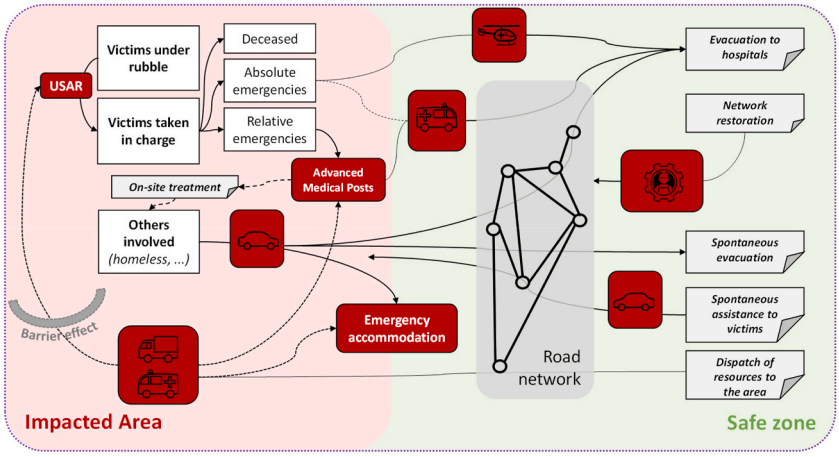

Fig. 1. Schematic representation of the main inflows and outflows to/from the impacted area during the initial response phase following the onset of an earthquake.

Table 2
Definition of main agents involved in the inflows and outflows (to/from the impacted area). Cells in italic represent actions that do not rely on the road network (i.e., airborne transportation with helicopters).

Type of response	Action	Who	When	Importance	Origin/ impacted area	Destination/ impacted area
Unorganized spontaneous reaction	Evacuating	Affected populations	Immediately	–	In	Out
	Going to hospitals	Injuries		–	In	Out
	Spontaneous assistance to victims	Citizens & Associations		–	Out	In
First aid	Providing assistance to victims	SAR		Extreme	Out	In
		First medical aid		Extreme	Out	In
	Securing the impacted area	Security forces (Police)		High	Out	In
	Evacuating injured people	*Rescue helicopters (rotations)*		*Extreme*	*Out ↔ In*	
		Ambulances (rotations)		High	Out	In
					In	Out
Building situational awareness	Assessing the situation with field reconnaissance	*Helicopters from civil protection*		*High*	*Out*	*In*
		Network and critical infrastructures operators	After a few hours	High	Out	In
Second aid & restoration	Providing assistance to affected populations	Local authorities NGOs, …		High	Out	In

structure is modelled to represent the contribution of intra- and inter-event error terms of the related ground-motion model (GMM) to the spatial distribution of the IMs at the various site (more details in Gehl et al. [28]).

- Damage state (DS) of the components, based on pre-selected seismic fragility curves and dependent on the IM level at the components' sites. Fragility curves take the form of a lognormal cumulative distribution function, characterized by a mean and a standard-deviation. If only two damage states are considered (i.e., component is functional or non-functional), the following convention is adopted: $DS = 1$ if the component is intact, $DS = 0$ if non-functional. The assumption of binary damage states is followed for the rest of the study. A similar assumption is adopted for road segments exposed to debris from collapsed buildings: if the road is blocked, it is considered as non-functional.
- Accessibility of a minimum link set (MLS) between two locations A and B of the road network. A MLS is defined as a minimum set of components whose joint survival ensures survival of the system (here, the connectivity between A and B). In the case of complex networks containing intersections or alternative routes, multiple MLSs exist between A and B, representing the number of different possible routes to reach the destination. By definition, a MLS represents a sub-system of components in series. The following

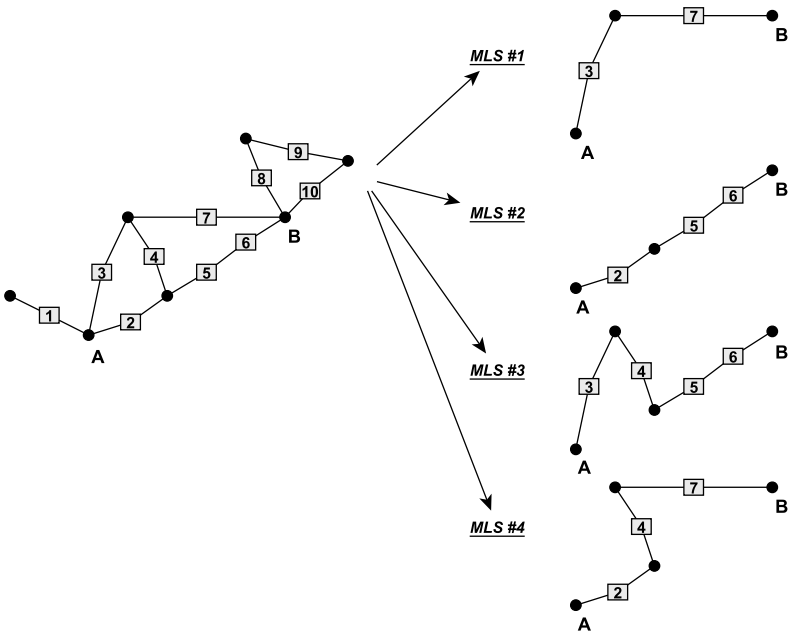

Fig. 2. Decomposition of the A-B routes into four MLSs, for an illustrative network. Black dots represent intersections in the network, and numbered rectangles represent components.

convention is adopted: $MLS = 1$ if the MLS is accessible and $MLS = 0$ if not. Therefore, for a given MLS k containing p components, the associated variable MLS_k is defined as follows: $MLS_k = DS_1$ x … x DS_p (in the case of binary damage states).

The decomposition of a road network into MLSs is illustrated in Fig. 2, where 4 MLSs are identified, each containing a different subset of components. Then, the corresponding BN may be built as shown in Fig. 3.

Two types of observations may be entered as evidence in the BN:

- Strong-motion recordings by seismic stations, which corresponds to evidence entered at the level of the IM variables;
- Identification of the damage states of some components, e.g. with near-real time structural monitoring [34], which corresponds to evidence entered at the level of the DS variables.

With the BN implemented in the OpenBUGS tool, the evidence is then propagated through the related variables. In the inference algorithm, several MCMC chains are initiated: each chain is built with a Gibbs sampling scheme, where variables are successively sampled from the posterior distribution of previous variables. As a result, the BN generates thousands of samples for all variables, which are then assembled to estimate their posterior distributions given the evidence. Examples of these realisations are provided in Table 3 and Table 4, where for a given earthquake event and related field observations, posterior statistics of variables of interest may be extracted from the BN inference.

From Tables 3 and 4, it is possible to extract damage and loss estimates in the form of probabilities, such as P ($DS_i = 0$) the probability of failure of component i, or P ($MLS_j = 0$) the probability of MLS j being inaccessible. While such raw mathematical results may be of little practical use to crisis managers, the following sections will demonstrate how they can lay a foundation for risk-informed decision making. Finally, it should be noted that while the present sub-section focuses on a BN approach to obtain posterior distributions of damages and losses at component- and system-level, other implementations are possible such as the generation of stochastic loss scenarios for instance [35]. The main objective remains to generate samples that may be organized as in Tables 3 and 4, in order to be exploited in the subsequent steps.

3.2. Identification of candidate routes and their related metrics

The rapid loss assessment outcomes obtained in the previous sub-section provide the probability that two locations A and B of the road network are disconnected (i.e., system performance measure S). However, it may be more useful to identify which actual routes to take in order to reach B from A, for instance in the light of the various constraints detailed in Table 2. The decomposition of the A-B connectivity into MLSs is very useful in this matter, since each MLS is equivalent to a possible different route to reach the destination. Starting from Table 4, it is straightforward to distinguish between two specific routes:

- the fastest (or shortest) route, which corresponds to the MLS with the smallest length of travel (or travel time, if a free-flow speed model is attributed to each segment of the road network);
- the safest route, which corresponds to the MLS with the highest probability of accessibility.

For each of these two choices, it is also useful to access an even higher resolution by examining the probability of failure of all components that are crossed when travelling from A to B, for the selected route R_0. For instance, assuming that MLS #2 is the fastest one in the network from Fig. 2, the analysis of Table 3 gives access to component failure probabilities P($DS_2 = 0$), P($DS_5 = 0$) and P($DS_6 = 0$). However, it would be more useful to know the probability that component i of the MLS is the first to be non-functional, when crossing the components in sequential order from A and B. In the illustrative example, this rationale translates to the quantification of the joint probabilities P($DS_2 = 0$), P($DS_2 = 1$, $DS_5 = 0$) and P($DS_2 = 1$, $DS_5 = 1$, $DS_6 = 0$). Such quantities are also easily extracted from Table 3 by counting the rows that contain the desired chain of 0s and 1s and by dividing the sum by n, the number of samples.

An even further level of analysis consists of looking at the back-up route R_1, in case that the i-th component along the initial route R_0 is the first one to be non-functional. However, instead of looking for alternative MLSs starting from the origin A, it is more efficient to

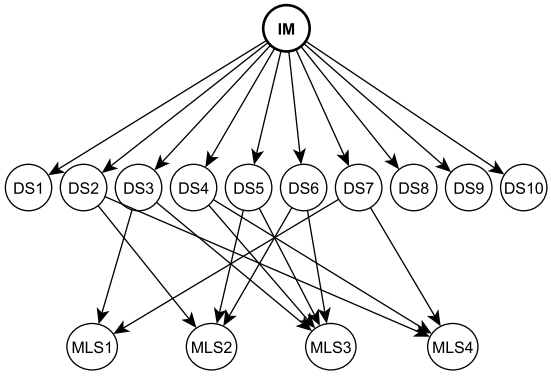

Fig. 3. BN corresponding to the illustrative example of Fig. 2. The node IM is in bold because it represents the vector of spatially correlated IMs at the sites. The nodes DS_1, …,DS_{10} correspond the damage states of the 10 components in the system.

Table 3
Illustrative example of n MCMC samples for the damage states of the 10 components in Fig. 2, assuming $DS_7 = 0$ (failure of component #7) as an evidence.

Sample #	DS_1	DS_2	DS_3	DS_4	DS_5	$DS1_6$	DS_7	DS_8	DS_9	DS_{10}
1	1	1	0	1	1	1	0	0	1	1
2	0	1	0	0	1	1	0	0	0	1
…	0	0	0	1	1	0	0	1	1	0
n	1	1	1	1	1	1	0	1	0	0

Table 4
Illustrative example of n MCMC samples for the accessibility of the 4 MLSs in Fig. 2, assuming $DS_7 = 0$ (failure of component #7) as an evidence.

Sample #	MLS_1	MLS_2	MLS_3	MLS_4
1	0	1	0	0
2	0	1	0	0
…	0	0	0	0
n	0	1	1	0

identify the MLSs that can be reached directly from component i, in order to reproduce the behaviour of a driver that would look for the closest deviation after encountering an obstacle along the initial route. The following algorithm is proposed in order to identify the back-up route:

- excluding the MLS corresponding to route R_0, only the other MLSs that contain the subset of components [1; …; i-1] from the initial MLS (i.e., associated with route R_0) are selected as candidates;
- if no MLS is found, the component subset is restricted to [1; …; i-2] and so on, until a set of alternative MLSs is found;
- among the alternative MLSs, the final part of each MLS (i.e., excluding the first part that is common with R_0) is evaluated depending on the initial selection criterion (i.e., fastest or safest route), in order to find the best fit for the back-up route R_1.

The procedure is illustrated in Fig. 4, where it is assumed that component #6 is found to be non-functional when travelling along route R_0 (MLS #2). No other MLS contains the components #2 and #5, therefore the algorithm identifies other MLSs containing component #2: MLS #4 is the only candidate and it is therefore selected as route R_1. Finally, a simple graph analysis is able to find the part of the route that must be travelled back once having encountered the non-functional component #6 in order to turn on the back-up route R_1. In such a hypothetical case, the total travel time to reach B is decomposed into three segments (see Fig. 4, right) assuming that a driver discovers first-hand that component #6 is not crossable: *(1)* travel time TT_1 to reach component #6 on route R_0, *(2)* travel time TT_2 to travel back and turn on back-up route R_1 and *(3)* travel time TT_3 to reach destination B via R_1.

As a result, for a given route R_0 associated with MLS #q containing k components arranged in sequential order, it is possible to systemically apply the above procedure to each component, in order to evaluate a set of metrics that may subsequently be used in decision making. These metrics are summarized in Table 5. For each line in the table (i.e., for each component failure event), there will always be three sets of travel times – the first (TT_1) corresponds to the original MLS as far as the first damaged component, the second (TT_2) corresponds to the connection between the damaged component and the back-up MLS, and the third (TT_3) corresponds to final part of R_1. TT_1 depends solely on the route R_0 and on the index of the failed component, while TT_2 and TT_3 depend also on the back-up MLS.

In Table 5, the last column, representing the probability that R_1 is not accessible, is a conditional probability given the knowledge of the damage states of the subset of components [1; …; i], since the driver has now access to first-hand information about the components they have already passed. Although this conditional probability could be quantified by solving again the BN with this new evidence, computation times are not compatible with a rapid response context. Another option is to exploit the initial simulation outcomes of Tables 3 and 4, such that only the rows that correspond to the correct values $DS_1 = 1, \ldots, DS_{i\text{-}1} = 1, DS_i = 0$ are kept and the combinations that result in the disconnection of MLS_j are counted, in order to compute the estimate of $P(MLS_j = 0 \mid \ldots, DS_{i\text{-}1} = 1, DS_i = 0)$. Selecting and counting rows from Tables 3 and 4 leads theoretically to the same results as solving again the BN, although the number of samples extracted from the tables may not be enough to reach stable estimates of the posterior distribution. The quantity P

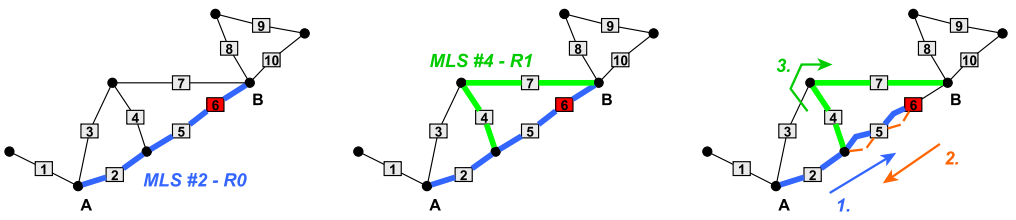

Fig. 4. Left: initial route R_0 (blue line) containing non-functional component #6 (red rectangle); middle: identification of back-up route R_1; right: sequence of travel to reach location B with the back-up route.

Table 5
For a given initial route R_0, evaluation of each component involved (i.e., probability that the given component is the first to be non-functional along the route) and the related consequences in terms of back-up route.

Component #	Probability that component is the first to fail	R_1	TT_1	TT_2	TT_3	Probability that R_1 is not accessible
…	…	…	…	…	…	…
i	P(…, $DS_{i\text{-}1} = 1$, $DS_i = 0$)	MLS #j	$TT_{1,i}(R_0)$	$TT_{2,i}(R_0, j)$	$TT_{3,i}(R_0, j)$	P($MLS_j = 0 \mid \ldots, DS_{i\text{-}1} = 1, DS_i = 0$)
…	…	…	…	…	…	…
k	P(…, $DS_{k\text{-}1} = 1$, $DS_k = 0$)	MLS #p	$TT_{1,k}(R_0)$	$TT_{2,k}(R_0, p)$	$TT_{3,k}(R_0, p)$	P($MLS_p = 0 \mid \ldots, DS_{k\text{-}1} = 1, DS_k = 0$)

($MLS_j = 0 \mid \ldots, DS_{i\text{-}1} = 1, DS_i = 0$) represents the probability that the back-up route R_1 turns out to be inaccessible as well, requiring the need to identify a second-order back-up route R_2, and so forth. In the present study, it has been decided to stop the recursion at R_1 in order to keep computations to a minimum and to simplify the outcomes. Therefore, the case in which neither R_0 nor R_1 are accessible may be seen as a situation where a connection between A and B is not guaranteed and where the driver is left without any rerouting information: in this case, the driver has to find another route on their own, outside the scope of the DSS.

First, it should be noted that the set of events $\{\ldots, DS_{i\text{-}1} = 1, DS_i = 0\}_{i=1..k}$ represents all possibilities regarding which component is the first to be found damaged. Therefore, these events are mutually exclusive and collectively exhaustive with respect to the disconnection of MLS #q, such that:

$$\sum_{i=1}^{k} P(\ldots, DS_{i-1} = 1, DS_i = 0) = P\left(MLS_q = 0\right) = 1 - P\left(MLS_q = 1\right) \tag{1}$$

Therefore, the probability that the route R_0 (associated to MLS #q) and its back-ups are inaccessible is expressed as follows:

$$\begin{aligned} P(R = 0) &= P(R_0 = 0, R_1 = 0) \\ &= 1 - P(R_0 = 1) - P(R_0 = 0, R_1 = 1) \\ &= 1 - P\left(MLS_q = 1\right) - P\left(MLS_q = 0, R_1 = 1\right) \\ &= 1 - P\left(MLS_q = 1\right) - P\left(R_1 = 1 \middle| MLS_q = 0\right) P\left(MLS_q = 0\right) \\ &= 1 - P\left(MLS_q = 1\right) - \sum_{i=1}^{k} P\left(MLS_j = 1 \middle| \ldots, DS_{i-1} = 1, DS_i = 0\right) P(\ldots, DS_{i-1} = 1, DS_i = 0) \end{aligned} \tag{2}$$

On the other hand, for a given route R_0 corresponding to MLS #q, without initial knowledge of the states of the components (except for the probabilities provided by the loss assessment tool), the expected value of the travel time $E[TT]$ may be expressed as follows:

$$E[TT] = P\left(MLS_q = 1\right) TT_0 + \sum_{i=1}^{k} P(\ldots, DS_{i-1} = 1, DS_i = 0)\left(TT_{1,i} + TT_{2,i} + TT_{3,i}\right) \tag{3}$$

where TT_0 is the travel time from A to B on route R_0 if all components along the route are functional. It should be noted that the expected travel time does not account for the potential functionality loss of the backup route, which constitutes a first term approximation when evaluating the travel time.

For each component i along the route R_0, the term P(…, $DS_{i\text{-}1} = 1, DS_i = 0$)($TT_{1,i} + TT_{2,i} + TT_{3,i}$) may be interpreted as an indicator of the criticality of the component, since it represents the probability of occurrence of an adverse event multiplied by its consequences. Such a measure is very useful to identify the most critical component(s) along the route and to launch targeted inspection operations, with the objective of reducing important uncertainties about travel conditions.

The two quantities defined in Eqs. (2) and (3) may finally be used as criteria to evaluate a given route, both in terms of reliability (probability of safe back-up options) and efficiency (expected travel time). Such metrics are then assembled into a consequence matrix [36] taking the form of a table that lists a set of possible actions, which are evaluated in the light of a set of criteria (quantifying the positive or negative impacts of each action). In the present case, various options are compared, such as the use of either the fastest or the safest route, or even the choice of multiple destinations (e.g., when a driver has to choose between different hospitals in the area). An example consequence matrix is presented in Table 6, which has to be related to the different use cases and their corresponding criteria detailed in Table 2.

Table 6
Example of consequence matrix adapted to the choice between possible initial routes $R_{0,i}$.

Action	C1 – Expected travel time E[TT]	C2 – Probability of both initial route and back-up routes to be inaccessible P($R_0 = 0, R_1 = 0$)
Take $R_{0,1}$ to B_1		
Take $R_{0,2}$ to B_1		
…		
Take $R_{0,3}$ to B_2		
Take $R_{0,4}$ to B_2		
…	…	…

3.3. Towards decision making

The rapid estimation of damages that may affect the usability of roads is essential for the selection of suitable routes that minimize travel times and the risk of encountering impassable structures due to failure. The consequence matrix presented in Section 3.2 does not allow a user to prioritize between different criteria. It is therefore necessary to establish a decision matrix that enables the different criteria (and related metrics) of the consequence matrix to be weighted in line with the priorities of each user. For this purpose, the formulation introduced by Yoon and Hwang [37] and applied by Cremen and Galasso [36] is used, where each value of the consequence matrix is first normalized as follows:

$$r_{I_i,C_j} = \frac{C_j^{I_i}}{\sqrt{\sum_{k=1}^{Na}\left(C_j^{I_k}\right)^2}} \tag{4}$$

where $r_{Ii,Cj}$ is the normalized value of the jth criterion for the ith action, C_j^{Ii} is the jth criterion value for the ith action, and Na is the number of actions.

Then, the decision matrix (Table 7) is constructed by weighting each $r_{Ii,}$ value according to stakeholder priorities toward each criterion, with w_1 being the weight attributed to expected travel-time, and w_2 the one attributed to the probability of backup failure.

As described by Cremen and Galasso [36], each action i (related to itinerary I_i) is evaluated via its score S_i, defined as follows:

$$S_i = \frac{y_i^-}{y_i^+ + y_i^-} \tag{5}$$

with:

$$y_i^+ = \sqrt{\sum_{j=1}^{2}\left[\left(min\left(r_{I_1,C_j}.\,w_j,\ \ldots,\ r_{I_{Na},C_j}.\,w_j\right) - \left(r_{I_i,C_j}w_j\right)\right]^2} \tag{6}$$

$$y_i^- = \sqrt{\sum_{j=1}^{2}\left[\left(max\left(r_{I_1,C_j}.\,w_j,\ \ldots,\ r_{I_{Na},C_j}.\,w_j\right) - \left(r_{I_i,C_j}w_j\right)\right]^2}, \tag{7}$$

where y_i^- and y_i^+ represent the total distance of action I_i with respect to the worst and best solution, respectively. The best action taking into account weights w_1 and w_2 assigned by the user is then the one maximizing the score value S_i. Here, min (Eq. (6)) and max (Eq. (7)) are respectively associated with the best and worst outcomes because the criteria of interest should both be minimised (expected travel time and probability of inaccessibility).

4. Application to a road network in France

This section describes the application of the DSS to a case-study area in the French Pyrenees mountain range. Results are provided for a set of arbitrary earthquakes.

4.1. Description of the case-study and modelling assumptions

The case-study area has been extensively described in the study by Gehl et al. [28]. It consists of a road network, which connects 53 municipalities (i.e., built areas) located in a valley around the town of Bagnères-de-Luchon (Pyrenees, France). It is assumed here that the road network under study consists of two vulnerable types of components:

- Bridges, i.e., the 118 bridges in Luchon Valley that can be directly damaged due to earthquakes and thus might become inaccessible and non-functional. Their characteristics (structural features, topology), and the corresponding fragility functions, are discussed in more details in Gehl et al. and Sun et al. [28,38]. The most common bridge type consists of short single-span bridges (length <50 m), followed by masonry arch bridges. In total, 18 different fragility curves have been assigned (3 models for the 83 single-span bridges, 3 for the 7 continuous multi-span bridges, and 12 for the 28 arch bridges), mostly taken from the SYNER-G database [39].
- Road segments, i.e., the roads nearby buildings in Bagnères-de-Luchon that might be blocked because of debris from collapsed buildings. These vulnerable segments are identified manually as road segments in Bagnères-de-Luchon that are adjacent to buildings. An inventory of the number of buildings associated with each of the vulnerable road segments has been carried out using Google Maps (see Fig. 5). More details on the procedure to estimate the probability of road blockage by debris of collapsed buildings

Table 7
Example of decision matrix adapted to the choice between possible routes.

Itinerary	Costs		Score
	C1 – Expected travel time (E[TT])	C2 – Probability of both initial route and back-up routes to be inaccessible (P($R_0 = 0, R_1 = 0$))	
I_1	$r_{I1,1}.\,w_1$	$r_{I1,2}.\,w_2$	S_1
…	…	…	…
I_{Na}	$r_{INa,1}.\,w_1$	$r_{INa,2}.\,w_2$	S_{Na}

are provided in Argyroudis et al. [10]. In the present case-study, a total of 17 road segments exposed to blockage by debris have been found.

Accounting for the 118 bridges and for the 17 road segments exposed to debris, there are 135 vulnerable components that are considered as part of the seismic performance assessment of the road network.

In the present case-study, it is assumed that the damaged area (i.e., most prone to require emergency support and relief) is concentrated in the downtown of Bagnères-de-Luchon (point A in Fig. 6) due its high density of population compared to other settlements. Four entrance and exit points of the network are assigned based on their proximity to support facilities (e.g., hospitals, emergency centres, etc.) outside of the network (see points B1 to B4 in Fig. 6). Therefore, the objective is to assess the connectivity between points A and B1, …., B4 in order to determine potential routes between the damaged area and support facilities. To this end, the MLSs between each pair of origins-destinations are identified:

- between A and B1: 820 MLSs;
- between A and B2: 2460 MLSs;
- between A and B3: 120 MLSs;
- between A and B4: 820 MLSs.

By definition, each MLS represents a unique itinerary between A and B*i*, therefore the identification of adequate routes is equivalent to evaluating MLSs in terms of length (travel time) and probability of accessibility.

The analysis of the surroundings of the road network has led to the identification of three hospitals (H1 to H3) and three resource centres (RC1 to RC3, representing fire and police stations). Depending on the existence of direct access roads, these support facilities are linked to the entrance and exit points of the physical road network through virtual edges (i.e., outer links that are considered to be always accessible and that are associated with a given travel time):

- H1, H2, H3 and RC1 are all linked to points B1, B2 and B3;
- RC2 and RC3 are both linked to points B1 and B4.

This configuration is summarized in Fig. 7.

The case-study area is located in a medium seismicity zone, according to the terminology adopted in the French seismic zonation [40]: this zone corresponds to the highest seismicity level in mainland France, with a reference peak ground acceleration on rock at 1.6

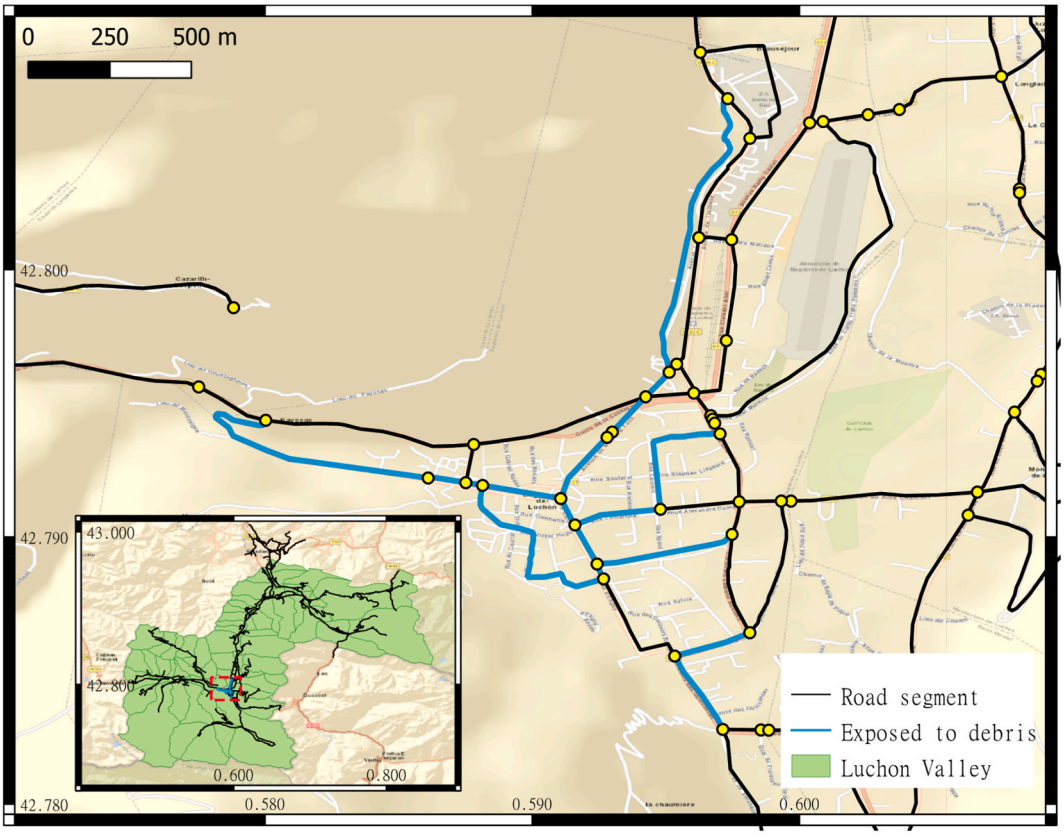

Fig. 5. Identification of built areas near roads in the downtown of Bagnères-de-Luchon.

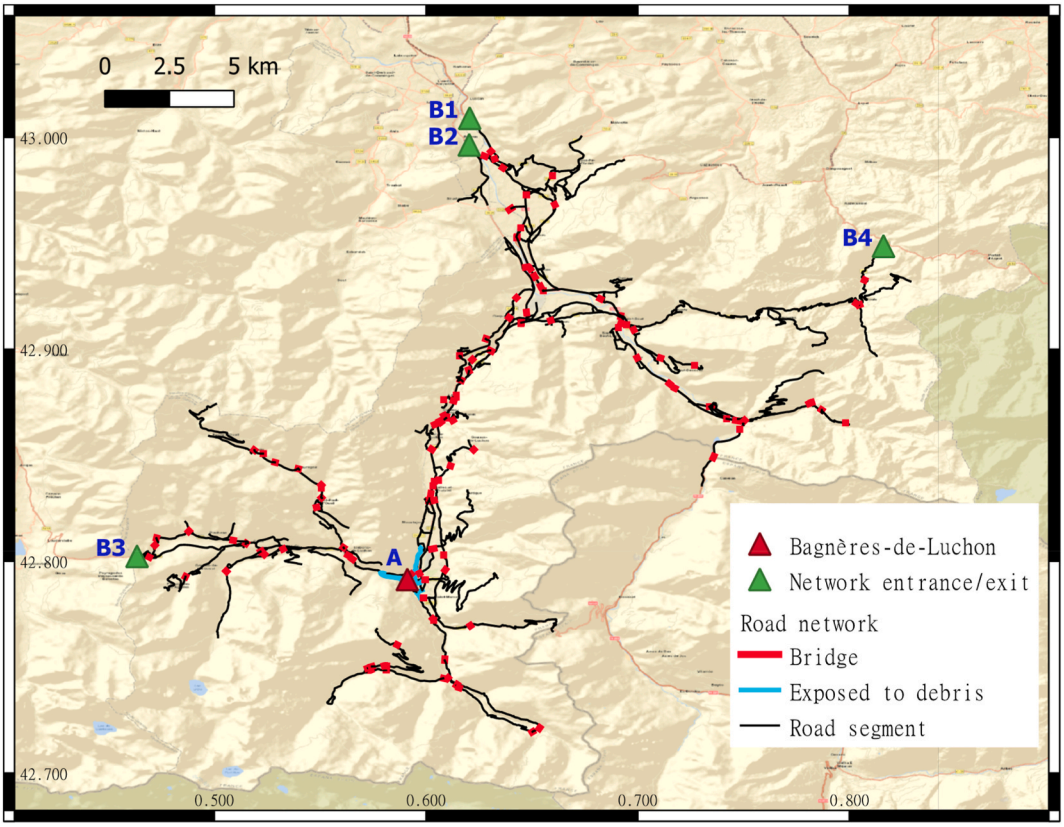

Fig. 6. Overview of the road network considered for the application of the DSS.

m/s^2 with a return period of 475 years. For the sake of demonstration, different arbitrary earthquake scenarios are conducted. Three potential epicentre locations are selected, located approximately 20 km from the barycentre of the road network, but with varying azimuth (EQ1, EQ2 and EQ3 in Fig. 7). A magnitude M_w 6.1 is assumed for all hypocentres with a shallow depth of 10 km. The magnitude of the scenarios events is in accordance with some of the largest historical earthquakes estimated in the area such as the M_w 6.5 earthquake in 1660 near Bagnères-de-Bigorre [41]. Their locations, in the foothills of the Pyrenees south of the Bagnères-de-Luchon valley and near the Spanish border, corresponds roughly to the epicentre area of most earthquakes in this region.

In order to exploit the loss updating capabilities of the Bayesian framework [28], hypothetical observations from 7 seismic stations and damage measures on 5 bridges are set as evidence in the BN (2 survivals and 3 failures). It is assumed that one of the monitored bridges belongs to the identified MLSs, and it has been observed as intact.

All selected fragility curves use PGA as IM; therefore, the regional GMM by Tapia [42] is applied here for the estimation of the prior distribution of IM. It uses only three parameters, namely the moment magnitude, the epicentral distance and the earthquake depth. For PGA, the spatial correlation model by Jayaram and Baker [43] is expressed as:

$$\rho_{ij} = exp\left(-\frac{3h}{8.5}\right) \tag{8}$$

where h is the inter-site distance in km.

Finally, site amplification factors are applied using the soil model by Roullé et al. [44].

4.2. *Strategies for improved decision making*

The weights introduced in the sub-section 3.3 may be defined by considering different first responder profiles, based on their action prioritization criteria. Three typical first responder profiles, each with different prioritization criteria (mostly related to first aiders), are considered as an example:

1. $w_1 = 0.75$; $w_2 = 0.25$: stakeholder having a strong preference for the fastest itinerary (criterion 1);
2. $w_1 = 0.25$; $w_2 = 0.75$: stakeholder having a strong preference for itineraries with a useable escape route (criterion 2);
3. $w_1 = w_2 = 0.5$: stakeholder having no preference between itineraries.

Considering the operational problem of the initial response phase described in Section 2, each of these three prioritization profiles have been arbitrarily assigned to first-responders contributing to first aid (Table 8): with respect to Table 2, the present study is limited

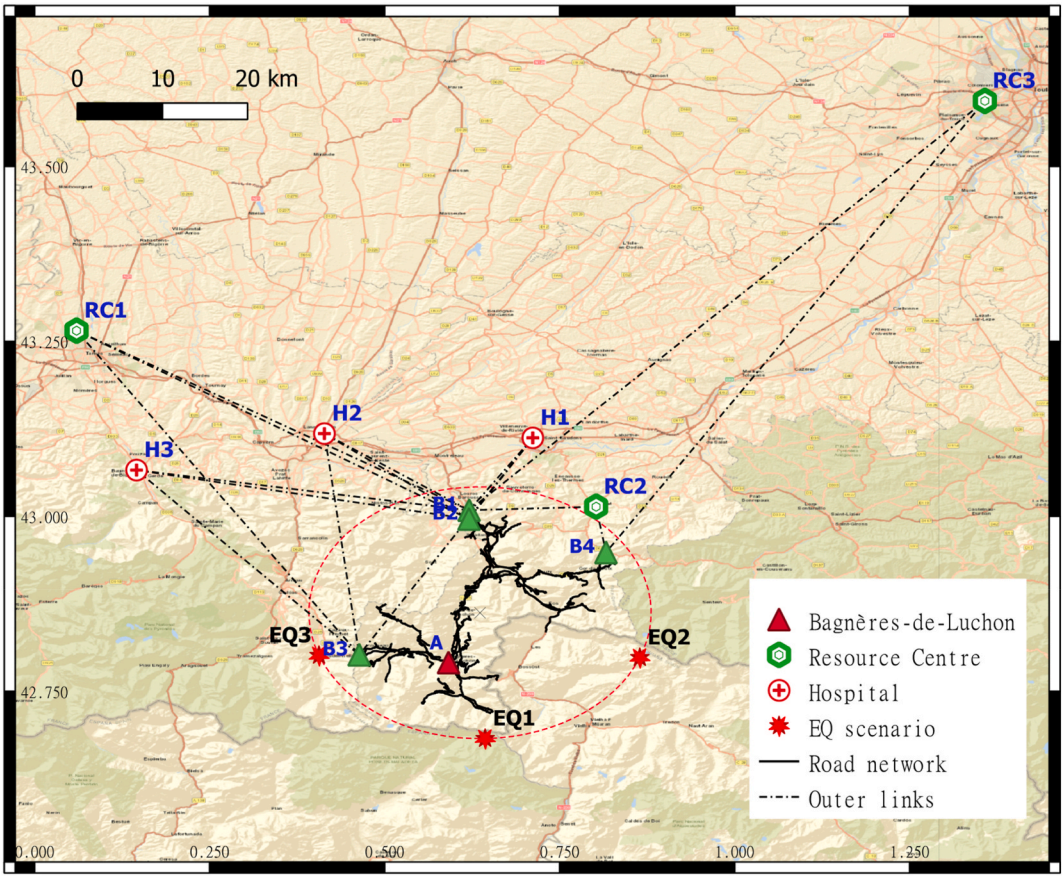

Fig. 7. Location of resource centres and hospitals with respect to the road network.

Table 8
Attribution of prioritization profiles to first-responders contributing to the first aid.

Who	Origin	Destination	Action	Prioritization profile
SAR teams	Fire station	Impacted area	Search and rescue of survivors	1
First medical aid	Hospital	Impacted area	Deploying AMPs	1
Security forces	Police station	Impacted area	Securing the impacted area	3
Ambulances	Ambulance depot	Impacted area	On-site provision of means for victim evacuation	2
	Impacted area	Hospital reachable with itinerary maximizing route score	Evacuation of a vital emergency	1
			Evacuation of a non-vital emergency	2

to the case of first aiders only (other users introduced in Table 2 are not considered). Thus, it is considered that all mobilized first-responders seek to reach the impacted area as quickly as possible, with the exception of the security forces to whom we assign a 'neutral' profile. Among the actors considered, only the ambulances have to rotate between the safe (external) zone and the impacted area, thus leading to a bidirectional problem. In order to illustrate the proposed methodological framework, two distinct behaviors are considered, depending on whether the ambulances have to evacuate injured people without vital urgency (profile 2) or seriously injured people who have to reach the hospital as soon as possible (profile 1).

5. Results

The system loss updating procedure [28] is applied to the earthquake scenarios defined in the previous sub-section, and the results are used to build the DSS for choosing adequate itineraries, given the profile of the users.

For instance, for earthquake scenario EQ1, assuming that the objective is to reach any hospital from the damaged area, a first level of analysis consists of identifying the fastest and safest itineraries (see Fig. 8):

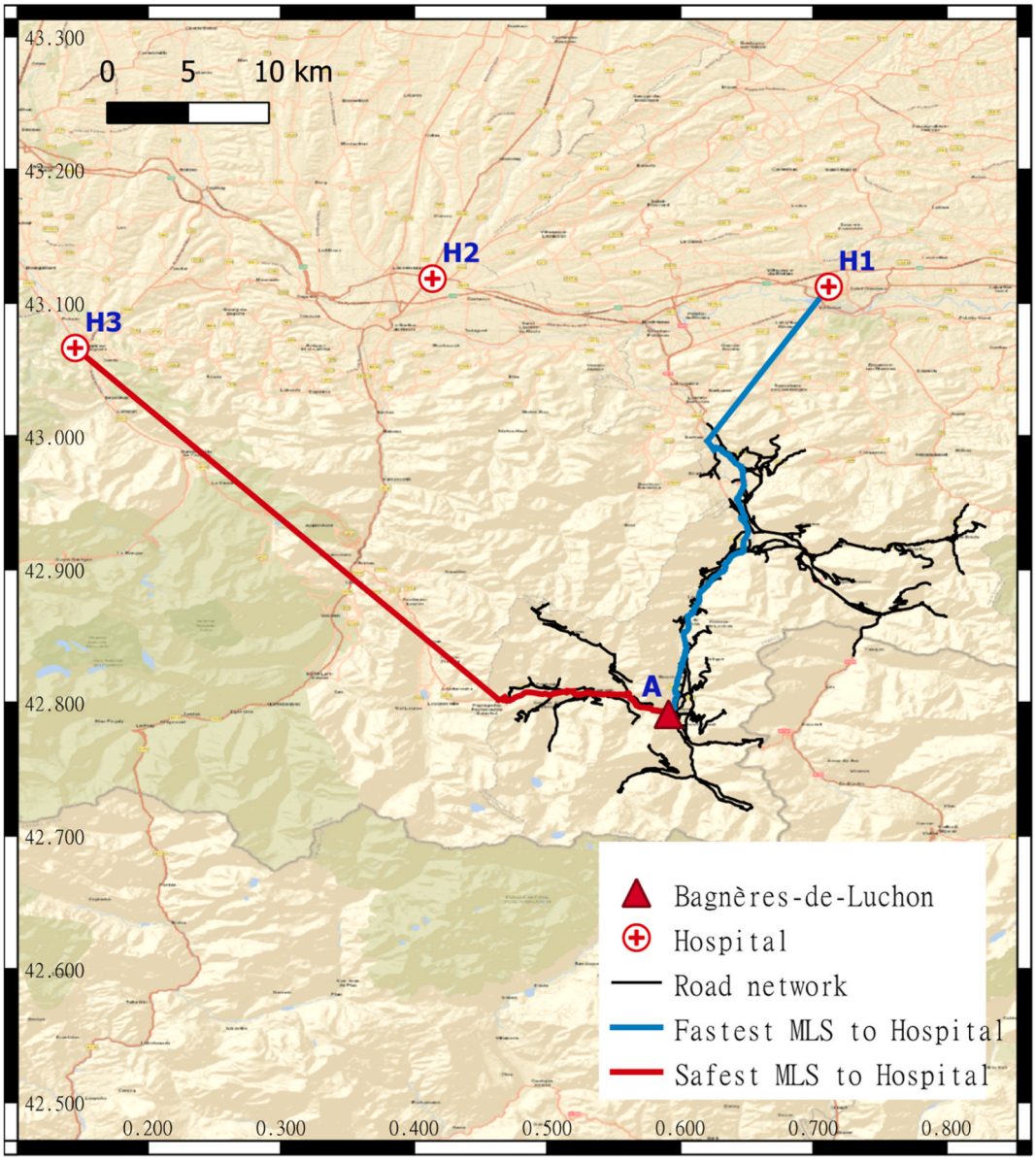

Fig. 8. Shortest and safest route options for travelling from A to a hospital in the case of earthquake scenario EQ1.

- fastest option: route B2\#29 (exiting the network at point B2, via MLS #29), with a travel time of 57 min and a probability of inaccessibility of 0.607;
- safest option: route B3\#55 (exiting the network at point B3, via MLS #55), with a travel time of 85 min and a probability of inaccessibility of 0.429.

Travel times are estimated by considering free-flow circulations, with a travel speed that matches the speed limits of the various road segments (i.e., between 50 km/h and 80 km/h in France).

Further analysing route B2\#29, the loss assessment outcomes provide the probability of failure of the 15 vulnerable components that compose the MLS (see Table 9) in sequential order. For each potential component failure, it is possible to estimate the consequences in terms of using the next best back-up MLS and of additional travel time to complete the journey. A close look at Table 9 reveals the depth added by the decomposition into sequential component failures: for instance, failures of components #609 and #360 both result in the selection of MLS B1\#60 as the back-up route, however the associated probability P(*backup MLS fails*) is different. This observation is due to two phenomena:

- the remaining portions of the backup MLS differ when component #360 is damaged versus when component #609 is damaged;

Table 9
Statistics for the route B2\#29, identified as the fastest option to travel from the damaged area to any hospital in the case of earthquake scenario EQ1. TT is the travel time in mins.

Component ID	P(*Component is first to fail*)	TT to reach first failed component (TT_1)	Backup MLS	P (*backup MLS fails*)	TT to catch backup MLS (TT_2)	TT of backup MLS (TT_3)
608	0.433	0.29	B1\#60	0.885	0.29	56.79
609	0.010	0.29	B1\#60	0.693	0.29	56.79
360	0.044	0.50	B1\#60	0.927	0.50	56.79
110	0.094	4.41	B1\#12	0.925	3.79	55.55
595	0.025	4.80	B1\#9	0.752	0.30	51.97
593	0.013	5.21	B1\#9	0.806	0.71	51.97
591	0.015	5.46	B3\#54	0.338	5.46	86.24
577	0.008	8.71	B1\#30	0.454	0.15	47.56
473	0.039	9.03	B1\#30	0.363	0.46	47.56
571	0.003	9.08	B1\#30	0.574	0.51	47.56
562	0.012	10.20	B3\#54	0.186	10.20	86.24
516	0.008	15.94	B1\#14	0.335	1.53	41.89
491	0.049	18.53	B2\#8	0.657	2.94	39.08
482	0.002	24.34	B1\#10	0.000	0.03	37.46
478	0.003	25.32	B1\#10	0.000	1.01	37.46

- when observing the failure of either component #360 or #609, the samples are updated based on this evidence, thus altering the failure probabilities of other components.

Therefore, one of the original features of the proposed approach consists in the damage updating of components, which allows for a progressive refinement of loss estimates in the area.

The extraction of the backup MLS and of the additional travel time to reach the backup from the initial route R_0 is illustrated in Fig. 9, considering the example of component #593 being the first to fail along the route.

Similar statistics as those shown in Table 9 are assembled for each fastest and safest route for each pair of origin and destination location for each earthquake scenario. The metrics presented in Eqs. (2) and (3) are detailed in Table 10 for each travel option. Following the various use-cases detailed in Table 2, the most important objectives are the travels from the damaged area to any of the hospitals and from each resource centre (e.g., fire and police stations) to the damaged area, if the study is limited to the consideration of first aid responders. Fastest routes tend to have smaller E(TT) value and higher P($R = 0$) values than safest routes. However, in some specific cases, E(TT) is larger for the fastest option than for the safest one (e.g., from RC3 to damaged area) because component failures along the fastest route may induce long detours to reach backup itineraries, while the choice of the safest route ensures that such occurrences are more limited. It is then interesting to note that what was initially selected as the fastest route (in undamaged conditions) may actually be longer when considering the impact of potential component failures. Therefore, because of such second-order effects, the initial selection of fastest and safest routes as possible actions may not consider all optimal solutions and it may lead to miss out on other routes with smaller travel time and/or the lower probability of inaccessibility: this limitation should be kept in mind when selecting route options.

Finally, the scoring procedure by Yoon and Hwang [37], also used by Cremen and Galasso [36], employing the user profiles defined in Section 3.3, is applied to the statistics detailed in Table 10, to quantify the scores of each travel option (see Table 11). In this example, it is considered that the three hospitals are interchangeable, such that the DSS must choose which hospital is the 'best' destination: as a result, all three hospitals are grouped into the same **Query 1** in Table 11. Conversely, when evaluating travel routes between resource centres and the damaged area, the starting point is fixed, therefore each pair of origin-destination locations [RC_i – A] becomes the object of a specific query (i.e., **Query 2 to 4** in Table 11).

From Table 11, the following observations can be made:

- The DSS is useful to identify the most adequate routes for each query depending on the user profile. Even for a relatively simple road network, a total of 6 routes were selected as preferred options:
  - o Route B3\#55: from damaged area to hospital, for all profiles in EQ1 and EQ2, and for profiles p2 and p3 in EQ3; from resource centre #1 to damaged area, for all profiles in all earthquake scenarios.
  - o Route B2\#29: from damaged area to hospital, for profile p1 in EQ3.
  - o Route B1\#64: from resource centres #2 and #3 to damaged area, for all profiles in EQ1.
  - o Route B1\#814: from resource centres #2 and #3 to damaged area, for all profiles in EQ2.
  - o Route B1\#812: from resource centre #2 to damaged area, for profiles p2 and p3 in EQ3; from resource centre #3 to damaged area, for all profiles in EQ3.
  - o Route B1\#10: from resource centre #2 to damaged area, for profile p1 in EQ3.
- Except for EQ3, the consideration of different user profiles has no large influence on the ranking of the options, although the scores are modified. More pronounced weighting between the different user profiles may lead to another ranking.
- The three earthquake epicentres are located at a similar distance from the barycentre of the road network, however they are grouped in the Southern part of the map in order to account for the seismotectonic context of the area. Another case-study with more diverse earthquake scenarios would result in more variety in terms of road network functionality and route selection.

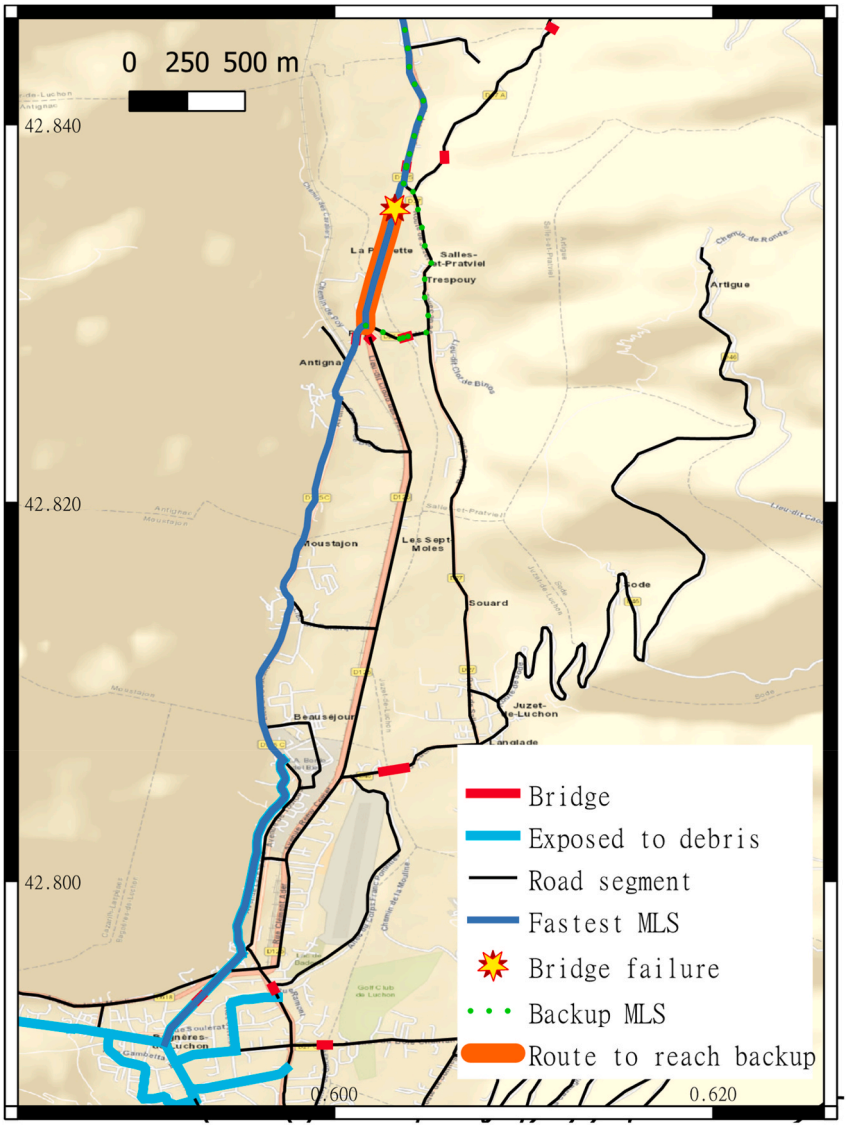

Fig. 9. Identification of the backup option of initial route B2\#29, in the case that component #593 (yellow star) is the first component to have failed along the route.

6. Conclusions

In the initial phase of emergency management, the problem of timely accessibility of the impacted area is particularly critical, with first-responders having to choose routes without information on which one will be the most efficient, while prioritizing different criteria. In this context, the methodology proposed here lays the foundations of a context-based user-centric DSS.

Although the results presented in the Pyrenean use-case show a low sensitivity of the route ranking both to the considered earthquake location and to user preferences, the proposed methodology successfully manages to account for user preferences related to prioritization of routes in a convenient DSS. It is worth noting that the considered case of a valley located in a piedmont area is probably less sensitive to the problem of route prioritization, as there are only a few entry/escape options. The situation might be different in a lowland region with more numerous and interconnected road networks. Furthermore, the criteria for route selection have been simplified here to only two parameters (relating to travel time and escape options in the case of impassable components), but other parameters could be considered depending on the specific problems of each stakeholder. For demonstration purposes, the present study has considered only two types of vulnerable components (i.e., bridges and roads exposed to debris from collapsed structures): in a mountainous area like the Bagnères-de-Luchon valley, many components such as embankments, retaining walls or roads exposed to earthquake-induced landslides should be included in the risk analysis, in order to reach a complete overview of accessibility issues during the post-earthquake phase. Moreover, the selected case-study area remains exposed to relatively modest seismicity levels when compared to other areas in Europe: therefore, it is currently difficult to validate the results with any recent damaging earthquakes. Further efforts should be devoted to the development of an application that relies on actual post-earthquake

Table 10
Evaluation of each identified route for each travel option with respect to the expected value of travel time in minutes (E[*TT*]) and the probability that both the route and its backup are not accessible (P[$R = 0$]) for each earthquake scenario.

Travel option		EQ1			EQ2			EQ3		
		E(*TT*)	P($R = 0$)	Route	E(*TT*)	P($R = 0$)	Route	E(*TT*)	P($R = 0$)	Route
From damaged area to hospital	Fastest to H1	57.17	0.61	B2 \#29	57.39	0.50	B2\#29	57.07	0.45	B2\#29
	Safest to H1	85.25	0.43	B3 \#55	85.81	0.22	B3\#55	83.21	0.37	B3\#55
	Fastest to H2	62.21	0.61	B2 \#29	62.18	0.50	B2\#29	61.93	0.45	B2\#29
	Safest to H2	61.18	0.43	B3 \#55	60.62	0.22	B3\#55	64.64	0.37	B3\#55
	Fastest to H3	73.26	0.46	B3 \#55	71.70	0.25	B3\#55	80.08	0.39	B3\#55
	Safest to H3	73.60	0.43	B3 \#55	72.01	0.22	B3\#55	82.10	0.37	B3\#55
From resource centre to damaged area	Fastest from RC1	133.82	0,461	B3 \#55	116.94	0.25	B3\#55	162.36	0.39	B3\#55
	Safest from RC1	134.23	0.45	B3 \#55	117.27	0.25	B3\#55	164.63	0.37	B3\#55
	Fastest from RC2	57.07	0,556	B1 \#10	57.63	0.48	B1\#10	57.04	0.42	B1\#10
	Safest from RC2	57.87	0.51	B1 \#64	59.88	0.34	B1 \#814	65.13	0.29	B1 \#812
	Fastest from RC3	209.27	0.74	B4\#3	290.25	0.83	B4\#3	189.83	0.57	B4\#3
	Safest from RC3	174.10	0.51	B1 \#64	182.83	0.34	B1 \#814	207.56	0.29	B1 \#812

Table 11
Scoring of the different travel options with respect to the three defined user profiles for each earthquake scenario. The bold cells represent the preferred options. User profiles are: p1 - stakeholder with a strong preference for the fastest itinerary; p2 - stakeholder with a strong preference for itineraries with a useable escape route; p3 - stakeholder with no preference between itineraries.

Travel option		Query	EQ1			EQ2			EQ3		
			S (p1)	S (p2)	S (p3)	S (p1)	S (p2)	S (p3)	S (p1)	S (p2)	S (p3)
From damaged area to hospital	Fastest to H1	1	0.77	0.27	0.53	0.61	0.15	0.34	**0.84**	0.36	0.63
	Safest to H1		0.23	0.73	0.47	0.39	0.85	0.66	0.16	0.64	0.37
	Fastest to H2		0.70	0.24	0.48	0.55	0.12	0.30	0.75	0.32	0.57
	Safest to H2		**0.86**	**0.95**	**0.90**	**0.91**	**0.98**	**0.95**	0.72	**0.87**	**0.76**
	Fastest to H3		0.46	0.74	0.58	0.60	0.86	0.76	0.18	0.57	0.34
	Safest to H3		0.47	0.82	0.63	0.61	0.92	0.80	0.17	0.65	0.38
From resource centre to damaged area	Fastest from RC1	**2**	0.33	0.05	0.14	0.22	0.03	0.08	0.44	0.08	0.20
	Safest from RC1		**0.67**	**0.95**	**0.86**	**0.78**	**0.97**	**0.92**	**0.56**	**0.92**	**0.80**
	Fastest from RC2	**3**	0.34	0.05	0.15	0.27	0.04	0.11	**0.54**	0.11	0.28
	Safest from RC2		**0.66**	**0.95**	**0.85**	**0.73**	**0.96**	**0.89**	0.46	**0.89**	**0.72**
	Fastest from RC3	**4**	0.00	0.00	0.00	0.00	0.00	0.00	0.30	0.05	0.13
	Safest from RC3		**1.00**	**1.00**	**1.00**	**1.00**	**1.00**	**1.00**	**0.70**	**0.95**	**0.87**

data, in order to validate the method and evaluate its benefits under real conditions.

In addition to the route selection function that accounts for the bespoke needs of a given stakeholder, the prospect of being able to update the model on the basis of field observations by the first-responders (for example via a dedicated web-app) is particularly interesting. First, it would allow – like online navigation services - to quickly improve route selection by progressively replacing the modelling of potential impacts on the road network with ground-truth observations. Secondly, it would allow authorities to quickly implement a robust traffic management plan by identifying the routes to prioritize according to the specific profiles of the different types of users.

Declaration of competing interest

The authors declare that they have no known competing financial interests or personal relationships that could have appeared to influence the work reported in this paper.

Acknowledgments

This research was funded by the European Union's Horizon 2020 research and innovation program, grant number 821046, project

TURNkey.

References

[1] M. Feltynowski, M. Langner, The role of EASeR project in enhancing search and rescue teams performance, Saf. Fire Technol. 53 (1) (2019).
[2] M.G. Durante, L. Di Sarno, P. Zimmaro, J.P. Stewart, Damage to roadway infrastructure from 2016 Central Italy earthquake sequence, Earthq. Spectra 34 (4) (2018) 1721–1737.
[3] JRC (Joint Research Centre), Institute for the protection and security of the citizen, Tsionis, G, in: U. Hancilar, F. Taucer, B. Khazai (Eds.), Guidelines for Typology Definition of European Physical Assets for Earthquake Risk Assessment, Publications Office, 2013. https://data.europa.eu/doi/10.2788/68751.
[4] FEMA, HAZUS-MH MR4 Technical Manual, Federal Emergency Management Agency, 2003.
[5] F. Freddi, C. Galasso, G. Cremen, A. Dall'Asta, L. Di Sarno, A. Giaralis, G. Woo, Innovations in earthquake risk reduction for resilience: recent advances and challenges, Int. J. Disaster Risk Reduc. 60 (2021), 102267.
[6] G. Tsionis, M.N. Fardis, Fragility functions of road and railway bridges, in: K. Pitilakis, H. Crowley, A.M. Kaynia (Eds.), SYNER-G: Typology Definition and Fragility Functions for Physical Elements at Seismic Risk, Springer, Dordrecht, 2014, pp. 259–297.
[7] S. Argyroudis, K. Pitilakis, Seismic fragility curves of shallow tunnels in alluvial deposits, Soil Dynam. Earthq. Eng. 35 (2012) 1–12.
[8] S. Argyroudis, A.M. Kaynia, Analytical seismic fragility functions for highway and railway embankments and cuts, Earthq. Eng. Struct. Dynam. 44 (11) (2015) 1863–1879.
[9] S. Argyroudis, A.M. Kaynia, K. Pitilakis, Development of fragility functions for geotechnical constructions: application to cantilever retaining walls, Soil Dynam. Earthq. Eng. 50 (2013) 106–116.
[10] S. Argyroudis, J. Selva, P. Gehl, K. Pitilakis, Systemic seismic risk assessment of road networks considering interactions with the built environment, Comput. Aided Civ. Infrastruct. Eng. 30 (7) (2015) 524–540.
[11] A.M. El-Maissi, S.A. Argyroudis, F.M. Nazri, Seismic vulnerability assessment methodologies for roadway assets and networks: a state-of-the-art review, Sustainability 13 (1) (2021) 61.
[12] L. Dueñas-Osorio, J.I. Craig, B.J. Goodno, Seismic response of critical interdependent networks, Earthq. Eng. Struct. Dynam. 36 (2) (2007) 285–306.
[13] S.E. Chang, M. Shinozuka, J.E. Moore, Probabilistic earthquake scenarios: extending risk analysis methodologies to spatially distributed systems, Earthq. Spectra 16 (3) (2000) 557–572.
[14] A. Kiremidjian, J. Moore, Y.Y. Fan, O. Yazlali, N. Basoz, M. Williams, Seismic risk assessment of transportation network systems, J. Earthq. Eng. 11 (3) (2007) 371–382.
[15] N. Jayaram, J.W. Baker, Efficient sampling and data reduction techniques for probabilistic seismic lifeline risk assessment, Earthq. Eng. Struct. Dynam. 39 (10) (2010) 1109–1131.
[16] C.S. Oliveira, M.A. Ferreira, F.M. de Sá, The concept of a disruption index: application to the overall impact of the July 9, 1998 Faial earthquake (Azores islands), Bull. Earthq. Eng. 10 (1) (2012) 7–25.
[17] P. Bocchini, D.M. Frangopol, Restoration of bridge networks after an earthquake: multicriteria intervention optimization, Earthq. Spectra 28 (2) (2012) 427–455.
[18] M. Miller, J.W. Baker, Coupling mode-destination accessibility with seismic risk assessment to identify at-risk communities, Reliab. Eng. Syst. Saf. 147 (2016) 60–71.
[19] W. Manopiniwes, T. Irohara, A review of relief supply chain optimization, Indus. Eng. Manag. Syst. 13 (1) (2014) 1–14.
[20] Y.J. Zheng, S.Y. Chen, H.F. Ling, Evolutionary optimization for disaster relief operations: a survey, Appl. Soft Comput. 27 (2015) 553–566.
[21] R. Faturechi, E. Miller-Hooks, Measuring the performance of transportation infrastructure systems in disasters: a comprehensive review, J. Infrastruct. Syst. 21 (1) (2015), 04014025.
[22] L. Chen, E. Miller-Hooks, Optimal team deployment in urban search and rescue, Transp. Res. Part B Methodol. 46 (8) (2012) 984–999.
[23] L. Ceferino, J. Mitrani-Reiser, A. Kiremidjian, G. Deierlein, C. Bambarén, Effective plans for hospital system response to earthquake emergencies, Nat. Commun. 11 (1) (2020) 1–12.
[24] B. Vitoriano, M.T. Ortuño, G. Tirado, J. Montero, A multi-criteria optimization model for humanitarian aid distribution, J. Global Optim. 51 (2) (2011) 189–208.
[25] I.I.D.A. Yasunori, F. Kurauchi, H. Shimada, Traffic management system against major earthquakes, IATSS Res. 24 (2) (2000) 6–17.
[26] G. Cremen, F. Bozzoni, S. Pistorio, C. Galasso, Developing a risk-informed decision-support system for earthquake early warning at a critical seaport, Reliab. Eng. Syst. Saf. 218 (2022), 108035.
[27] Y. Iida, F. Kurauchi, H. Shimada, Traffic management system against major earthquakes, IATSS Res. 24 (2) (2000) 6–17.
[28] P. Gehl, R. Fayjaloun, L. Sun, E. Tubaldi, C. Negulescu, E. Ozer, D. D'Ayala, Rapid earthquake loss updating of spatially distributed systems via sampling-based Bayesian inference, Bull. Earthq. Eng. (2022), https://doi.org/10.1007/s10518-022-01349-4.
[29] M. Bensi, A. Der Kiureghian, D. Straub, Efficient Bayesian network modeling of systems, Reliab. Eng. Syst. Saf. 112 (2013) 200–213.
[30] M. Bensi, A. Kiureghian, D. Straub, Framework for post-earthquake risk assessment and decision making for infrastructure systems, ASCE-ASME J. Risk Uncertain. Eng. Syst. Part A: Civ. Eng. 1 (1) (2015), 04014003.
[31] F. Cavalieri, P. Franchin, P. Gehl, D. D'Ayala, Bayesian networks and infrastructure systems: computational and methodological challenges, in: P. Gardoni (Ed.), Risk and Reliability Analysis: Theory and Applications, Springer, 2017.
[32] P. Gehl, F. Cavalieri, P. Franchin, Approximate Bayesian network formulation for the rapid loss assessment of real-world infrastructure systems, Reliab. Eng. Syst. Saf. 177 (2018) 80–93.
[33] D. Lunn, D. Spiegelhalter, A. Thomas, N. Best, The BUGS project: evolution, critique and future directions (with discussion), Stat. Med. 28 (2009) 3049–3082.
[34] E. Tubaldi, E. Ozer, J. Douglas, P. Gehl, Examining the contribution of near real-time data for rapid seismic loss assessment of structures, Struct. Health Monit. (2021) 1–20, https://doi.org/10.1177/1475921721996218.
[35] F. Cavalieri, P. Franchin, P. Gehl, B. Khazai, Quantitative assessment of social losses based on physical damage and interaction with infrastructural systems, Earthq. Eng. Struct. Dynam. 41 (11) (2012) 1569–1589.
[36] G. Cremen, C. Galasso, A decision-making methodology for risk-informed earthquake early warning, Comput. Aided Civ. Infrastruct. Eng. 36 (6) (2021) 747–761.
[37] K.P. Yoon, C.-L. Hwang, Multiple Attribute Decision Making: an Introduction, Sage Publications, 1995.
[38] L. Sun, D. D'Ayala, R. Fayjaloun, P. Gehl, Agent-based Model on Resilience-Oriented Rapid Responses of Road Networks under Seismic Hazard, Reliability Engineering & System Safety, 2021, p. 108030.
[39] H. Crowley, M. Colombi, V. Silva, R. Monteiro, S. Ozcebe, M. Fardis, G. Tsionis, P. Askouni, Fragility functions for roadway bridges, in: SYNER-G Deliverable Report D3 vol. 6, 2011.
[40] Journal Official, Décret n° 2010-1254 du 22 october 2010 relatif à la prévention du risque sismique, 2010. https://www.legifrance.gouv.fr/jorf/jo/2010/10/24/0248.
[41] K. Manchuel, P. Traversa, D. Baumont, M. Cara, E. Nayman, C. Durouchoux, The French seismic CATalogue (FCAT-17), Bull. Earthq. Eng. 16 (6) (2018) 2227–2251.
[42] M. Tapia, Desarrollo Y Aplicación de Métodos Avanzados Para La Caracterización de La Respuesta Sísmica Del Suelo a Escala Regional Y Local, Universidad Politécnica de Catalunya, Barcelona, Spain, 2006. PhD thesis.
[43] N. Jayaram, J.W. Baker, Correlation model for spatially distributed ground-motion intensities, Earthq. Eng. Struct. Dynam. 38 (15) (2009) 1687–1708.
[44] A. Roullé, A. Macau, S. Figueras, D. Monfort, N. Lantada, T. Susagna, J. Irizarry, Performing seismic scenario in the Luchon - Val d'Aran area, central Pyrenees, in: Proc. Of EUROGEO 2012, 2012 (Bolonia, Italy).